VNU Journal of Science: Mathematics – Physics, Vol. 40, No. 3 (2024) 97-105

VNU Journal of Science: Mathematics - Physics

Journal homepage: https://js.vnu.edu.vn/MaP

Original Article

Exciton Mott Transition in Photoexcited Semiconductor Revealed in Terahertz Absorption Spectra

Le Thi Hai Yen*

VNU University of Science, 334 Nguyen Trai, Thanh Xuan, Hanoi, Vietnam

Received 24 May 2024
Revised 15 June 2024; Accepted 02 July 2024

Abstract: We theoretically investigated the terahertz (THz) absorption spectra in optically excited semiconductors. By applying Bardeen-Cooper-Schriffer (BCS)-like mean field approximation, we have reproduced the spectral position of component originating from the 1s to 2p intraband transition in various density regimes. We have investigated the THz absorption spectra in various density regimes, and in a range of temperatures above the critical temperature of BCS-BEC crossover. By analysing THz absorption spectra, we have shown that the exciton Mott transition can be studied.

Keywords: Terahertz Spectroscopy, Exciton Mott transition, Semiconductors, Exciton.

1. Introduction

The issue of the exciton Mott transition has been studied for several decades [1, 2]. Beyond its fundamental interests, understanding several physical properties around the exciton Mott transition point is particularly important to develop novel high-performance optoelectronic devices such as highly efficient semiconductor laser diodes. This is because strong Coulomb correlations predominate around the transition point, which is a precursor for the optical gain by the *e-h* plasma. In fact, it has been shown both experimentally [3] and theoretically [4, 5] that the strong Coulomb correlation significantly modifies the optical absorption and gain spectra in quasi-one-dimensional semiconductors.

Recent developments in terahertz (THz) techniques attract much interest because of a wide range of applications in the fields of materials science [6], communication [7], and biotechnologies [8]. From the viewpoint of condensed matter physics, the THz time domain spectroscopy (THz-TDS) is ideally suited to measure conductivity of metals, semiconductors as well as phase transitions in these materials since they reflect and absorb THz radiation [9]. Furthermore, since the ponderomotive energy of THz radiation

* Corresponding author.
E-mail address: lethihaiyen@hus.edu.vn

https//doi.org/10.25073/2588-1124/vnumap.4943

for a given laser intensity is larger than that of visible light, we can apply strong electric fields (≈ 1 MV cm^{-1}) using a single-cycle THz pulse [10-12]. Therefore, THz techniques pave the new way for studying extreme nonlinear phenomena such as the impact ionization [12] and the high-order harmonic generation [6] in condensed matters, which cannot be analyzed with the perturbation theory.

Because of the extraordinary long lifetime (≃ 1 ms), 1s paraexcitons of the yellow series in Cu_2O have been studied to observe Bose-Einstein condensation (BEC) of excitons [13, 14]. The phonon assisted photoluminescence (PL) spectra was fitted to the Bose-Einstein distribution function to estimate density and temperature [15, 16]. However, the small radiative efficiency makes it difficult to experimentally determine their effective mass and lifetime. In order to circumvent the difficulty, THz absorption accompanied by the intraexciton transition from 1*s* to 2*p* states is proposed to be observed [17]. This is the counterpart of the Lyman spectroscopy in atomic hydrogen [18, 19], and is particularly useful because intraexcitonic transitions induced by the THz absorption are independent of the selection rules of optical transitions [20, 21]. Furthermore, they measure the coupling between 1s exciton ground state and higher relative momentum states, which independent of the center-of-mass momentum of excitons.

In this research, we aim at theoretically investigating the exciton Mott transition (density ionization) in optically excited direct bandgap bulk semiconductors with analyzing THz absorption spectra for various *e-h* pair densities.

2. Formulation

2.1. Model Hamiltonian

For the purpose of theoretically investigating exciton Mott transition with analyzing the THz absorption spectra in optically excited semiconductors, we formulate the THz absorption as the linear response of the semiconductor. In this study, we consider a three-dimensional *e-h* system in a direct bandgap bulk semiconductor, which consists of an isotropic and non-degenerate parabolic conduction and valence bands. Our model Hamiltonian is expressed in the form:

$$H_{tot} = H_{e-h} + H_1(t) + H_2(t) \tag{1}$$

where, H_{e-h}, H_1, and H_2 are the electron-hole Hamiltonian, the interaction Hamiltonian between particles and pump light, and the interaction Hamiltonian between particles and probe radiation, respectively. In this study, we consider an *e-h* system, which consists of conduction and valence bands. Hence, the *e-h* Hamiltonian can be expressed in two-band approximation:

$$H_{e-h} = \sum_{\boldsymbol{k}} \sum_{a} E_{\boldsymbol{k}a} {c^{\dagger}}_{\boldsymbol{k}a} c_{\boldsymbol{k}a} + \frac{1}{2} \sum_{\boldsymbol{k},\boldsymbol{p},\boldsymbol{q}} \mathcal{V}_{\boldsymbol{q}}\, c^{\dagger}_{\boldsymbol{k}+\boldsymbol{q}a} c^{\dagger}_{\boldsymbol{p}-\boldsymbol{q}b} c_{\boldsymbol{p}b} c_{\boldsymbol{k}a} \tag{2}$$

$$\begin{aligned} H_1(t) = &-\frac{e}{m_0} \sum_{\boldsymbol{k}} \sum_{ab} \boldsymbol{A}(t) \cdot \boldsymbol{P}_{ab}(\boldsymbol{k})(1-\delta_{ab}) {c^{\dagger}}_{\boldsymbol{k}a} c_{\boldsymbol{k}b} \\ &-\frac{e}{m_0} \sum_{\boldsymbol{k}} \sum_{a} [\boldsymbol{k} + \boldsymbol{P}_{aa}(\boldsymbol{k})] \cdot \boldsymbol{A}(t) {c^{\dagger}}_{\boldsymbol{k}a} c_{\boldsymbol{k}a} \end{aligned} \tag{3}$$

$$H_2(t) = \frac{e^2}{2m_0} \sum_{\boldsymbol{k}} \sum_{a} \boldsymbol{A}^2(t) {c^{\dagger}}_{\boldsymbol{k}a} c_{\boldsymbol{k}a} \tag{4}$$

where, c_{ka} is the annihilation operator of electrons with band a $(a = 1, 2)$, and lattice momentum $\boldsymbol{k}$.

The single-particle energies of electrons in the conduction band and holes in the valence band are given by $E_{k1} = \frac{k^2}{2m_e} + E_g - \mu_e$, and $E_{k2} = \frac{k^2}{2m_h} - \mu_h$, respectively, where E_g is bandgap energy between conduction and valence bands, m_e (m_h) is effective mass of electron (hole), respectively. The bare Coulomb interaction is $\mathcal{V}_q = 4\pi e^2/(\epsilon_0 q^2 L^3)$, where, ϵ_0 is the background dielectric constant of the unexcited crystal, and L^3 is the volume of the system. We have defined $\boldsymbol{P}_{ab}(\boldsymbol{k}) \equiv \frac{1}{V_0}\int_{V_0} d^3x\, u^*_{\boldsymbol{k}a}(\boldsymbol{x})(-i\nabla)u_{\boldsymbol{k}b}(\boldsymbol{x})$, where V_0 and $u_{\boldsymbol{k}a}(\boldsymbol{x})$ are the volume of the unit cell and the lattice periodic function, respectively. The first term on the right-hand side of H_1 describes the interband transition, while the second term and H_2 represent the intraband transition. We have employed the long wavelength approximation in which the $\boldsymbol{x}$-dependence of the vector potential is neglected; this approximation is justified when we investigate the optical or THz response where the wavelength of the radiation field is sufficiently long comparing with the lattice constant of the semiconductor crystal (dipole approximation).

In this study, THz absorption is calculated semi-classically, the THz field is given by the vector potential $A_{\boldsymbol{q}}(t)$. With the Coulomb gauge condition ($\nabla \cdot \boldsymbol{A} = 0$), the interaction Hamiltonian between carriers and THz field is

$$H_2 = -\frac{1}{V}\sum_{\boldsymbol{q},\lambda}(-1)^{\lambda-1} J^{\lambda}_{\boldsymbol{q}}(t)\, A^{\lambda}_{-\boldsymbol{q}}(t) \tag{5}$$

where $J^{\lambda}_{\boldsymbol{q}}(t) = \boldsymbol{e}^{\lambda}_{\boldsymbol{q}} \cdot \boldsymbol{J}_{\boldsymbol{q}}(t)$ and $A^{\lambda}_{-\boldsymbol{q}}(t) = \boldsymbol{e}^{\lambda}_{\boldsymbol{q}} \cdot \boldsymbol{A}_{\boldsymbol{q}}(t)$ are transverse components of the intraband current density operator and the vector potential, respectively. The linear polarization vectors $\boldsymbol{e}^{\lambda}_{\boldsymbol{q}}$ ($\lambda = 1, 2$) are defined so that $\left(\boldsymbol{e}^1_{\boldsymbol{q}}, \boldsymbol{e}^2_{\boldsymbol{q}}, \boldsymbol{q}/|\boldsymbol{q}|\right)$ forms a right-handed set of orthonormal vectors. Using the electron-hole representation, the intraband current operator is expressed as follows,

$$\begin{aligned}\boldsymbol{J}(t) = \frac{e}{m_0}\sum_{\boldsymbol{k}}\sum_{ab}(1-\delta_{ab}) c^{\dagger}{}_{\boldsymbol{k}a} c_{\boldsymbol{k}b} + e\sum_{a}\sum_{\boldsymbol{k}}\frac{\partial E_{\boldsymbol{k}a}}{\partial \boldsymbol{k}} c^{\dagger}{}_{\boldsymbol{k}a} c_{\boldsymbol{k}a} \\ -\frac{e^2}{2m_0}\boldsymbol{A}(t)\sum_{\boldsymbol{k}}\sum_{a} c^{\dagger}{}_{\boldsymbol{k}a} c_{\boldsymbol{k}a}\end{aligned} \tag{6}$$

here, for convenient we have defined as,

$$j^{\lambda}_{\boldsymbol{q}} \equiv e\sum_{\boldsymbol{k}}\sum_{a}\left(\boldsymbol{e}^{\lambda}_{\boldsymbol{q}} \cdot \frac{\partial E_{a\boldsymbol{k}}}{\partial \boldsymbol{k}}\right) c^{\dagger}{}_{\boldsymbol{k}a} c_{\boldsymbol{k}a} \tag{7}$$

Based on the BCS-like mean field theory, we introduce the mean-fields $\chi^{\mu}_{\boldsymbol{k}}$, with mean-field Hamiltonian which is involved in electron-hole Hamiltonian,

$$H_m = \sum_{\mu=0}^{3}\sum_{\boldsymbol{k}}\chi^{\mu}_{\boldsymbol{k}}\left(c^{\dagger}_{\boldsymbol{k}}\boldsymbol{\tau}^{\mu} c_{\boldsymbol{k}}\right) \tag{8}$$

here, τ^0 and τ^j ($j = 1, 2, 3$) are 2×2 unit matrix and the Pauli matrices, respectively. Then *e-h* Hamiltonian H_{e-h} is decomposed into two parts

$$H_{e-h} = H'_0 + H'_1$$

where, Hamiltonians H'_0 and H'_1 are defined as

$$H'_0 = \sum_{\boldsymbol{k}}\left(\mathcal{E}^{\mu}_{\boldsymbol{k}} + \chi^{\mu}_{\boldsymbol{k}}\right)\left(c^{\dagger}_{k}\tau^{\mu} c_{k}\right), \tag{9}$$

$$H_1' = \frac{1}{2}\sum_{ab}\sum_{\boldsymbol{kpq}} \mathcal{V}_{\boldsymbol{ka}}\, c_k^\dagger c_k^\dagger c_k c_k - \sum_{\boldsymbol{k}} \chi_k^\mu \left(c_k^\dagger \tau^\mu c_k\right)$$

In this analysis, we consider the screening effect in the static long wavelength limit with the static Single Plasmon Pole Approximation (SPPA). In this approximation the original Coulomb potential has been replaced by the potential defined as $V_{\boldsymbol{q}} = 4\pi e^2/\left(\epsilon_q q^2 L^3\right)$, where ϵ_q is static longitudinal dielectric function considering the static SPPA.

We also assuming that each particle in the *e-h* system moves in a single-particle potential that comes from its average interaction with all of the other particles. To employ the mean-field approximation in our calculation, we need to determine the mean-field χ_k^μ by solving the BCS-like gap equation that is obtained by a variational method. For this purpose, we introduce Bogoliubov transformation, which is often used to diagonalize Hamiltonians, in order to yield the steady-state solutions of the corresponding Schrödinger equation.

$$c_{\boldsymbol{k}} = u_{\boldsymbol{k}}\alpha_k + v_k\beta_{-k}^\dagger\,,\;\; d_{-\boldsymbol{k}} = u_k\beta_{-k} - v_k\alpha_k^\dagger \tag{10}$$

where α_k and β_{-k} are the annihilation operators of Bogoliubov quasiparticles, $u_{\boldsymbol{k}}$ and v_k are Bogoliubov parameters.

The mean-fields χ_k^μ are determined by the stationary condition of the functional,

$$\mathcal{F} = -T\ln Tr\left(e^{-\frac{H_0'}{T}}\right) + \langle\langle H_1'\rangle\rangle + \lambda\sum_{\boldsymbol{k}}\left[\langle\langle\left(c_{\boldsymbol{k}}^\dagger\boldsymbol{\tau}^0 c_{\boldsymbol{k}}\right)\rangle\rangle - 1\right] \tag{11}$$

where $\langle\langle \ldots \rangle\rangle$ denotes the statistical average defined by the Hamiltonian H_0'. The Lagrange multiplier λ is introduced to impose the charge neutrality condition, $\sum_k \langle\langle c_{\boldsymbol{k1}}^\dagger c_{\boldsymbol{k1}} - c_{\boldsymbol{k2}}c_{\boldsymbol{k2}}^\dagger\rangle\rangle = 0$.

That gives the following self-consistent equations for the Hartree-Fock self-energies

$$\begin{gathered}\chi_{\boldsymbol{k}}^0 = -\frac{1}{2}\sum_{\boldsymbol{p}} V_{\boldsymbol{k-p}}\left[F_{\boldsymbol{p}}^{(+)} - 1\right]; \quad \chi_{\boldsymbol{k}}^3 = -\frac{1}{2}\sum_{\boldsymbol{p}} V_{\boldsymbol{k-p}}F_{\boldsymbol{p}}^{(-)}\frac{\left(\mathfrak{E}_{\boldsymbol{p}}^3 + \chi_{\boldsymbol{p}}^3\right)}{E_{\boldsymbol{p}}''} \\ \chi_{\boldsymbol{k}}^1 + i\chi_{\boldsymbol{k}}^2 = -\frac{1}{2}\sum_{\boldsymbol{p}} V_{\boldsymbol{k-p}}F_{\boldsymbol{p}}^{(-)}\left[\frac{\chi_{\boldsymbol{p}}^1 + i\chi_{\boldsymbol{p}}^2}{E_{\boldsymbol{p}}''}\right]\end{gathered} \tag{12}$$

where, $\chi_{\boldsymbol{k}}^0 + \chi_{\boldsymbol{k}}^3$ $(\chi_{\boldsymbol{k}}^0 - \chi_{\boldsymbol{k}}^3)$ is the Hartree–Fock self-energy of conduction (valence) band electrons, $\chi_{\boldsymbol{k}}^1 + i\chi_{\boldsymbol{k}}^2$ is the order parameter of the *e-h* BCS state.

2.2. Transverse Dielectric Function

To investigate the exciton Mott transition in the THz absorption spectra, we are going to calculate the transverse dielectric function. The equation for the transverse dielectric function is obtained from Maxwell's equations and is expressed in the current density operator related to the interaction between carriers and THz field.

$$\left[\varepsilon_{\boldsymbol{q}}(\omega) - 1\right]E^\lambda(q,\omega) = -\frac{4\pi}{\omega^2}\int_{-\infty}^{+\infty} dt e^{i\omega t}\frac{\partial J^\lambda(q,t)}{\partial t} \tag{13}$$

Regarding the radiation-matter interaction Hamiltonian $H_1(t) + H_2(t)$ as the perturbation, then the transverse dielectric function can be calculated using the linear response theory, and the result is

$$\varepsilon_{\boldsymbol{q}}(\omega) = 1 - \frac{4\pi e^2}{m\omega^2}\mathcal{N}_{free} + \frac{4\pi i e^2}{\omega^2}\mathcal{G}_{\boldsymbol{q}}(\omega) \tag{14}$$

where, $\mathcal{G}_{\boldsymbol{q}}(\omega)$ is the Fourier transform of current-current correlation function

$$\mathcal{G}_{\boldsymbol{q}}(t) \equiv -i\theta(t)\left\langle\left[j_{\boldsymbol{q}}^{\lambda}(t), j_{-\boldsymbol{q}}^{\lambda}(0)\right]\right\rangle \tag{15}$$

Here $\langle \dots \rangle$ stands for the quantum statistical average with the density operator $\rho = \exp[-\beta\mathcal{K}]/Z$ where $Z \equiv \mathrm{Tr}\exp[-\beta\mathcal{K}]$ with $\mathcal{K} \equiv H_{e-h} - \sum_{\boldsymbol{k}}\sum_a \mu_a c^{\dagger}{}_{\boldsymbol{k}a}c_{\boldsymbol{k}a}$; $\mathcal{N}_{free}$ is the density of ionized plasma which plays an important role to conductivity, and $m = m_e m_h/(m_e + m_h)$ is the reduced mass of *e-h* pairs.

Applying Bogoliubov transformation current-current correlation function $\mathcal{G}_{\boldsymbol{q}}(t)$ becomes

$$\mathcal{G}_{\boldsymbol{q}}(t) = \sum_{\mu=0}^{3}\sum_{\nu=0}^{3}\sum_{\boldsymbol{k},\boldsymbol{p}}\left(\boldsymbol{k}\cdot\boldsymbol{e}_{\boldsymbol{q}}^{\lambda}\right)\left(\boldsymbol{p}\cdot\boldsymbol{e}_{\boldsymbol{q}}^{\lambda}\right)K_{\boldsymbol{k}}^{\mu}\Pi_{\boldsymbol{k},\boldsymbol{p}}^{\mu\nu}(t)K_{\boldsymbol{p}}^{\nu} \tag{16}$$

where the four-component vector, $K_{\boldsymbol{k}}^{0} \equiv \frac{1}{m_e} - \frac{1}{m_h}$; $K_{\boldsymbol{k}}^{1} \equiv \frac{2u_k v_k}{m}$; $K_{\boldsymbol{k}}^{2} \equiv 0$; $K_{\boldsymbol{k}}^{3} \equiv \frac{(u_k^2+v_k^2)}{m}$. The 4×4 matrix correlation function $\Pi_{\boldsymbol{k},\boldsymbol{p}}^{\mu\nu}(t)$ is defined as

$$\Pi_{\boldsymbol{k},\boldsymbol{p}}^{\mu\nu}(t) \equiv -i\theta(t)\langle\left[e^{iHt}\left(\phi_{\boldsymbol{k}}^{\dagger}\boldsymbol{\tau}^{\mu}\phi_{\boldsymbol{k}}\right)e^{-iHt}, \left(\phi_{\boldsymbol{p}}^{\dagger}\boldsymbol{\tau}^{\nu}\phi_{\boldsymbol{p}}\right)\right]\rangle \tag{17}$$

where $\phi_{\boldsymbol{k}} = \begin{pmatrix}\alpha_k^{\dagger}\\ \beta_{-k}\end{pmatrix}$ is the two-component operator in Nambu presentation, the Nambu pseudo spinor. And we introduce a convenient auxiliary function

$$\Psi_{\boldsymbol{k}}^{\mu}(t) = 2\sum_{\boldsymbol{p}}\left(\boldsymbol{p}\cdot\boldsymbol{e}_{\boldsymbol{q}}^{\lambda}\right)u_{\boldsymbol{p}}v_{\boldsymbol{p}}\Pi_{\boldsymbol{k},\boldsymbol{p}}^{\mu 1}(t) \tag{18}$$

By employing the simple time-dependent Hartree-Fock approximation (TDHFA), we assume that two particles propagate independently

$$\begin{aligned}\langle\left[\phi_{\boldsymbol{k}}^{\dagger}\phi_{\boldsymbol{p}}^{\dagger}\phi_{\boldsymbol{q}}\phi_{\boldsymbol{r}}, \phi_{\boldsymbol{s}}^{\dagger}\phi_{\boldsymbol{t}}\right]\rangle &\\ \simeq \langle\phi_{\boldsymbol{k}}^{\dagger}\phi_{\boldsymbol{r}}\rangle\langle\left[\phi_{\boldsymbol{p}}^{\dagger}\phi_{\boldsymbol{q}}, \phi_{\boldsymbol{s}}^{\dagger}\phi_{\boldsymbol{t}}\right]\rangle - \langle\phi_{\boldsymbol{k}}^{\dagger}\phi_{\boldsymbol{q}}\rangle\langle\left[\phi_{\boldsymbol{p}}^{\dagger}\phi_{\boldsymbol{r}}, \phi_{\boldsymbol{s}}^{\dagger}\phi_{\boldsymbol{t}}\right]\rangle &\\ + \langle\phi_{\boldsymbol{p}}^{\dagger}\phi_{\boldsymbol{q}}\rangle\langle\left[\phi_{\boldsymbol{k}}^{\dagger}\phi_{\boldsymbol{r}}, \phi_{\boldsymbol{s}}^{\dagger}\phi_{\boldsymbol{t}}\right]\rangle - \langle\phi_{\boldsymbol{p}}^{\dagger}\phi_{\boldsymbol{r}}\rangle\langle\left[\phi_{\boldsymbol{k}}^{\dagger}\phi_{\boldsymbol{q}}, \phi_{\boldsymbol{s}}^{\dagger}\phi_{\boldsymbol{t}}\right]\rangle &\end{aligned} \tag{19}$$

We obtain the equation of motion in the form of Bethe-Salpeter equations for Fourier transform of auxiliary function $\Psi_{\boldsymbol{k}}^{\mu}(t)$ as follow

$$\begin{aligned}-i\omega\Psi_{\boldsymbol{k}}^{1}(\omega) + 2iE_{\boldsymbol{k}}''\Psi_{\boldsymbol{k}}^{2}(\omega) &= -iF_{\kappa}^{(-)}\sum_{j=1,2}\sum_{\boldsymbol{p}}V_{\boldsymbol{k}-\boldsymbol{p}}C_{\boldsymbol{k},\boldsymbol{p}}^{2}\Psi_{\boldsymbol{p}}^{2}(\omega)\\ i\omega\Psi_{\boldsymbol{k}}^{2}(\omega) + 2iE_{\boldsymbol{k}}''\Psi_{\boldsymbol{k}}^{1}(\omega) &\\ = -iF_{\boldsymbol{k}}^{(-)}\sum_{j=1,2}\sum_{\boldsymbol{p}}V_{\boldsymbol{k}-\boldsymbol{p}}C_{\boldsymbol{k},\boldsymbol{p}}^{1}\Psi_{\boldsymbol{p}}^{1}(\omega) &+ 4u_{\boldsymbol{k}}v_{\boldsymbol{k}}\langle\phi_{\boldsymbol{k}}^{\dagger}\boldsymbol{\tau}^{3}\phi_{\boldsymbol{k}}\rangle\left(\boldsymbol{k}\cdot\boldsymbol{e}_{\boldsymbol{q}}^{\lambda}\right)\end{aligned} \tag{20}$$

Based on the equation-of-motion of dielectric function and the set of equation derived we have developed the numerical computation programs to numerically calculate THz absorption spectra.

3. Results and Discussion

In the numerical analysis, we have used the units where the exciton Rydberg energy E_0 and Botlzmann constant k_B is unity. Following the previous works, [22-25] we have calculated the exciton density by using material parameters of 1s paraexcitons in Cu_2O, in which exciton Bohr radius a_0 = 0.74

nm for the low energy state, the effective mass of electron (hole) 0.99 m_0 (0.58 m_0), and E_0 = 174 *meV*. Since this work is on the BCS-like pairing theory, we can investigate the THz absorption spectra in macroscopic quantum state, i.e., the Bose-Einstein condensed (BEC) state of excitons in low density state and exciton phase in high density regime.

However, in this work we focus on the case when carrier temperature T satisfying $E_0 > T > T_c$, where T_c is the critical temperature of the BCS – BEC crossover.

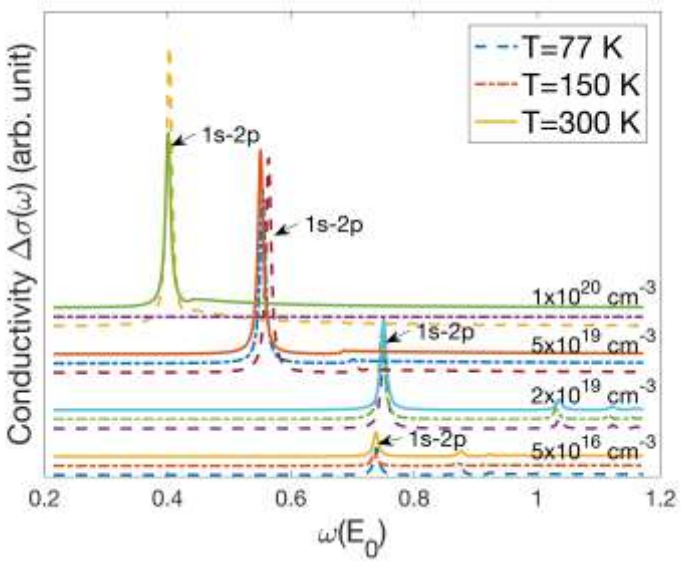

Figure 1. Conductivity spectra at various *e-h* density at different temperature T.

In Fig. 1, we show the conductivity spectra at various density regimes of *e-h* pairs in different temperature ranges. The sharp structures originate from the THz absorption which is accompanied by the intraexciton transition from 1s to 2p, 3p, ect. states. The broad absorption band due to the intraexciton transition from 1s to continuum state which is corresponding to ionized system. That is the evidence of the insulator-to-metal transition in optically excited semiconductor. The experiment in Cu_2O [26] has observed the THz spectral components originating from 1s to 2p, 3p, etc. states. As shown in the Fig. 1, the spectral position of the intraexciton transitions is almost unchanged in the investigating range of temperature. This behavior can be well explained by considering the temperature dependence of *e-h* pair density in the Fig. 2(a), *e-h* pair density is almost independent of temperature. It agrees with the previous work [25], that is the spectral position of the 1s-2p transition almost independent of density up to 3×10^{19} cm^{-3}. We also found that the spectral components shift towards lower energy as density $\mathcal{N}$ increasing. The sharp peak structures due to transitions from 1s to 4p, 3p, and 2p gradually disappear. Eventually, the exciton structures in the THz absorption spectra disappear at high density regime, i.e., the exciton Mott transition occurs.

In the Fig. 2 (c, d) we show the temperature dependence of Fermi momentum and the Coulomb-hole self-energy (Debye shift). Both Fermi momentum and Coulomb-hole energy hardly change as changing temperature. As their definitions, the state-filling effect measured by the Fermi momentum, and screening effect expressed in Coulomb-hole self-energy $\mathcal{D} \equiv \frac{1}{2}\sum_{\boldsymbol{p}}[\mathcal{V}_{\boldsymbol{p}} - V_{\boldsymbol{p}}]$, where $\mathcal{V}_{\boldsymbol{p}}$ ($V_{\boldsymbol{p}}$) is the bare (screened) Coulomb energy. They well explain the behavior of temperature dependence of *e-h* density and therefore the behavior of THz absorption spectra mentioned above is reasonable. The same behavior

is founded in temperature dependence of effective gap, that is corresponding to the least transition energy from 1s to ionization continuum, as shown in the Fig. 2(b). We have to mention that the density of the ionized plasma significantly contributes to reductions of exciton binding energy.

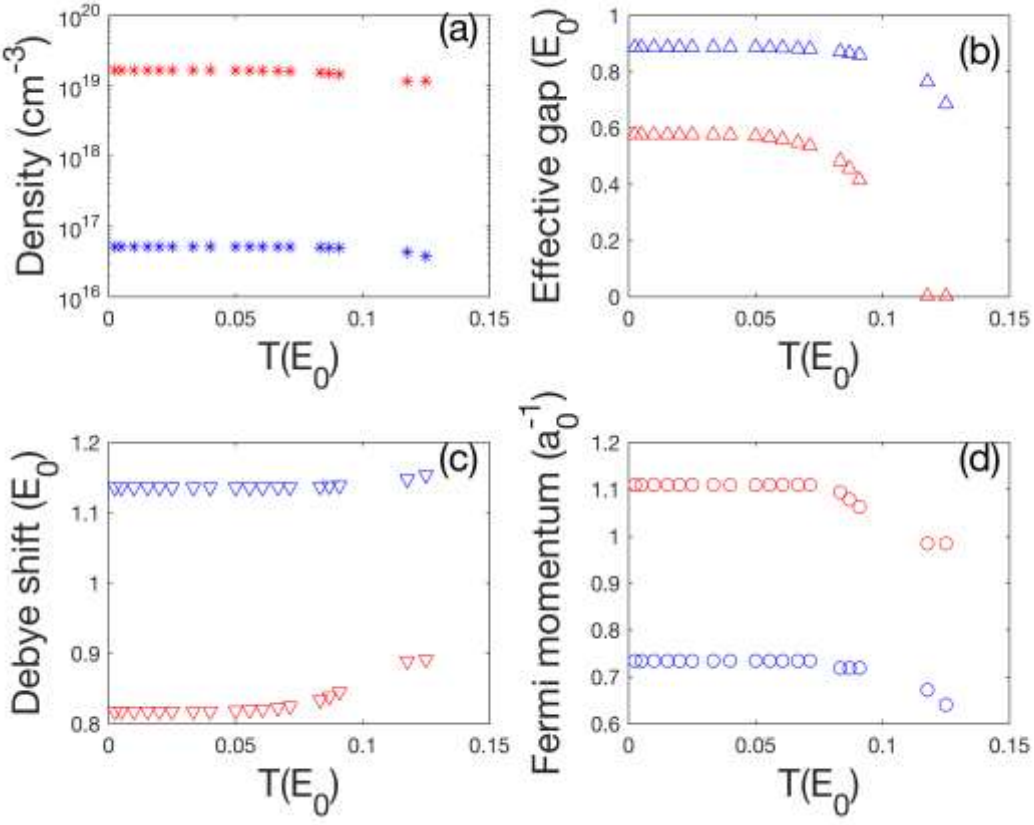

Figure 2. (a) Temperature dependence of e-h pair density. (b, c, d) Temperature dependence of effective gap, Debye shift (the Coulomb-hole self-energy), and Fermi momentum at various e-h density regimes, respectively.

4. Conclusion

In summary, we have analyzed both density dependence and temperature dependence of THz absorption spectra in photoexcited semiconductors above the critical temperature of BCS-BEC crossover, and have shown that it can clearly study exciton Mott transition. It is shown that our present theory qualitatively explains the density and temperature dependence of the THz absorption spectra in comparing with experimental results. However, the present theory cannot explain the phenomena of increase in the linewidth near the exciton Mott transition point, and several behaviors observed in experiments [28-31]. These points are interesting not only in device application but also in fundamental physics. This problem will be considered by a study based on the approach of self-consistent T-matrix in a forthcoming work.

Acknowledgments

The author would like to express her thank to Professor Takeshi J. Inagaki for fruitful comments. This research is funded by University of Science, Vietnam National University, Hanoi under project number TN.23.05.

References

[1] N. F. Mott, The Transition to the Metallic State, Philos. Mag., Vol. 6, No. 62, 1961, pp. 287-309, https://doi.org/10.1080/14786436108243318

[2] N. F. Mott, Metal-Insulator Transitions, Taylor and Francis, London, UK, 1974.

[3] Y. Hayamizu, M. Yoshita, Y. Takahashi, H. Akiyama, C. Z. Ning, L. N. Pfeifer, K. W. West, Biexciton Gain and the Mott Transition in GaAs Quantum Wires, Phys. Rev. Lett., Vol. 99, No. 16, 2007, pp. 167403, https://doi.org/10.1103/PhysRevLett.99.167403.

[4] T. Yoshioka, K. Asano, Exciton-Mott Physics in a Quasi-One-Dimensional Electron-Hole System, Phys. Rev. Lett., Vol. 107, No. 25, 2011, pp. 256403, https://doi.org/10.1103/PhysRevLett.107.256403.

[5] T. Yoshioka, K. Asano, Classical-quantum Crossoovers in Quasi-one-dimensional Electron-hole Systems: Exciton Mott Physics and Interband Optical Spectra, Phys. Rev. B, Vol. 86, No. 11, 2012, pp. 115314, https://doi.org/10.1103/PhysRevB.86.115314.

[6] R. A. Kaindl, M. A. Carnahan, D, Hägele, R. Lövenich, D. S. Chemla, Ultrafast Terahertz Probes of Transient Conducting and Insulating Phases in an Electron-hole Gas, Nature, Vol. 423, No. 20, 2003, pp. 734-738, https://doi.org/10.1038/nature01676.

[7] D. Saeekia, Handbook of Terehertz Technology for Imaging, Sensing and Communications, Woodhead Publishing, Cambridge, UK, 2013.

[8] X. Yin, B. W. H. Ng, D. Abbott, Terahertz Imaging for Biomedical Applications: Pattern Recognition and Tomographic Reconstruction. Springer, New York, 2012.

[9] E. Hendry, F. Wang, J. Shan, T. F. Heinz, M. Bonn, Electron Transport in TiO_2 Probed by THz Time-domain Spectroscopy, Phys. Rev. B, Vol. 69, No. 8, 2004, pp. 081101, https://doi.org/10.1103/PhysRevB.69.081101.

[10] H. Hirori, M. Nagai, K. Tanaka, Efficient Matrix-product State Method for Periodic Boundary Conditions, Phys. Rev. B, Vol. 81, No. 8, 2010, pp. 081305, https://doi.org/10.1103/PhysRevB.81.081103.

[11] H. Hirori, A. Doi, F. Blanchard, K. Tanaka, Single-cycle Terahertz Pulses with Amplitudes Exceeding 1 MV/cm Generated by Optical Rectification in $LiNbO_3$, Appl. Phys. Lett., Vol. 98, 2011, pp. 091106, https://doi.org/10.1063/1.3560062.

[12] M. Vanexter, C. Fattinger, D. Grischkowsky, Terahertz Time-domain Spectroscopy of Water Vapor, Opt. Lett., Vol. 14, No. 20, 1989, pp. 1128-1130, https://doi.org/10.1364/OL.14.001128.

[13] S. A. Moskalenko, D. W. Snoke, Bose-Einstein Condensation of Excitons, Cambridge University Press, Cambridge, England, 2000.

[14] A. Griffin, D. W. Snoke, S. Stringari, Bose-Einstein Condensation, Cambridge University Press, Cambridge, England, 1995.

[15] D. W. Snoke, J. P. Wolfe, A. Mysyrowicz, Evidence for Bose-Einstein Condensation of Excitons in Cu2O, Phys. Rev. B, Vol. 41, No. 16, 1990, pp. 11171, https://doi.org/10.1103/PhysRevB.41.11171.

[16] J. L. Lin, J. P. Wolfe, Bose-Einstein Condensation of Paraexcitons in Stressed Cu_2O, Phys. Rev. Lett., Vol. 71, No. 8, 1993, pp. 1222, https://doi.org/10.1103/PhysRevLett.71.1222.

[17] K. Johnsen, G. M. Kavoulakis, Probing Bose-Einstein Condensation of Excitons with Electromagnetic Radiation, Phys. Rev. Lett., Vol. 86, No. 5, 2001, pp. 858, https://doi.org/10.1103/PhysRevLett.86.858.

[18] H. Haken, On the Theory of Excitons in Solids, J. Phys. Chem. Solids, Vol. 8, 1959, pp. 166-171, https://doi.org/10.1016/0022-3697(59)90307-5.

[19] S. Nikitine, On the Possibility of Observation and the Intensity of (nn′) and (nn) Transitions between Exciton States in Cu_2O, J. Phys. Chem. Solids, Vol. 45, No. 8-9, 1984, pp. 949-954, https://doi.org/10.1016/0022-3697(84)90138-0.

[20] M. Jörger, E. Tsitsishvili, T. Flek, C. Klingshirn, Infrared Absorption by Exciton in Cu_2O, Phys. Stat. Sol. B, Vol. 238, No. 3, 2003, pp. 470-473, https://doi.org/10.1002/pssb.200303164.

[21] M. Jörger, T. Flek, C. Klingshirn, 1s→2p Terahertz Transitions of the 1s Paraexciton in Cu_2O, J. Lumin., Vol. 112, No. 1-4, 2005, pp. 21-24, https://doi.org/10.1016/j.jlumin.2004.09.041.

[22] T. J. Inagaki, T. Iida, M. Aihara, Many-body Theory of Pump-probe Spectra for Highly Excited Semiconductors, Phys. Rev. B, Vol. 62, No. 16, 2000, pp. 10852, https://doi.org/10.1103/PhysRevB.65.205204.

[23] T. J. Inagaki, M. Aihara, Many-body Theory for Luminescence Spectra in High-density Electron-hole Systems, Phys. Rev. B, Vol. 65, No. 20, 2002, pp. 205204, https://doi.org/10.1103/PhysRevB.65.205204.

[24] T. J. Inagaki, M. Aihara, Infrared Absorption in High-density Electron-hole Systems: The Role of Quantum Fluctuations, Phys. Rev. B, Vol. 66, No. 7, 2002, pp. 075204, https://doi.org/10.1103/PhysRevB.66.075204.

[25] Y. T. H. Le, T. J. Inagaki, Densitty Dependence of the Terahertz Absorption Spectra in Optically Excited Semiconductors, Phys. Sta. Sol. B, Vol. 253, No. 3, 2015, pp. 589-599, https://doi.org/10.1002/pssb.201451191.

[26] T. Tayagaki, A. Mysyrowicz, M. K. Gonokami, The Yellow Excitonic Series of Cu_2O Revisited by Lyman Spectroscopy, J. Phys. Soc. Jpn., Vol. 74, No. 5, 2015, pp. 1423-1426, https://doi.org/10.1143/JPSJ.74.1423.

[27] T. Suzuki, R. Shimano, Exciton Mott Transition in Si Revealed by Terahertz Spectroscopy, Phys. Rev. Lett., Vol. 109, No. 4, 2012, pp. 046402, https://doi.org/10.1103/PhysRevLett.109.046402.

[28] P. Nozières, S. S. Rink, Bose Condensation in an Attractive Fermion Gas: from Weak to Strong Coupling Superconductivity, J. Low Temp. Phys., Vol. 59, 1985, pp. 195-211, https://doi.org/10.1007/BF00683774.

[29] D. Kremp, D. Semkat, K. Henneberger, Quantum Condensation in Electron-hole Plasmas, Phys. Rev. B., Vol. 78, No. 12, 2008, pp. 125315, https://doi.org/10.1103/PhysRevB.78.125315.

[30] K. Yoshioka, E. Chae, M. K. Gonokami, Transition to a Bose-Einstein Condensate and Relaxation Explosion of Excitons at sub-Kelvin Temperatures, Nature Commun, Vol. 2, 2011, pp. 328, https://doi.org/10.1038/ncomms1335.

[31] H. Stolz, R. Schwartz, F. Kieseling, S. Som, M. Kaupsch, S. Sobkowiak, D. Semkat, N. Naka, T. Koch, and H. Fehske, Condensation of Excitons in Cu_2O at Ultracold Temperatures: Experiment and Theory, New J. Phys., Vol. 14, 2012, 105007, https://doi.org/10.1088/1367-2630/14/10/105007.

[32] H. Stolz, R. Zimmermann, Correlated and a Mass Action Law in Two-component Fermi Systems Excitons in an Electron-hole Plasma, Phys. Sta. Sol. B, Vol. 94, No. 1, 1979, pp. 135-146, https://doi.org/10.1002/pssb.2220940114.

[33] R. Zimmermann, H. Stolz, The Mass Action Law in Two-Component Fermi Systems Revisited Excitons and Electron-Hole Pairs, Phys. Sta. Sol. B, Vol. 131, No. 1, 1985, pp. 151-164, https://doi.org/10.1002/pssb.2221310115.

[34] N. H. Kwong, G. Rupper, R. Binder, Self-consistent T-matrix Theory of Semiconductor Light-absorption and Luminescence, Phys. Rev. B, Vol. 79, No. 15, 2009, pp. 155205, https://doi.org/10.1103/PhysRevB.79.155205.